ChemPubSoc Europe

DOI: 10.1002/open.201800120

ChemistryOPEN Full Papers

Synthesis of Hollow Co–Fe Prussian Blue Analogue Cubes by using Silica Spheres as a Sacrificial Template

Alowasheeir Azhar[+, a, b, c] Mohamed B. Zakaria[+,*a, b, d] El-Zeiny M. Ebeid,[d] Toyohiro Chikyow,[b] Yoshio Bando,[b] Abdulmohsen Ali Alshehri,[e] Yousef Gamaan Alghamdi,[e] Ze-Xing Cai,[b] Nanjundan Ashok Kumar,[f] Jianjian Lin,*[a] Hansu Kim,*[g] and Yusuke Yamauchi*[f, h]

Herein, we report a novel method for the formation of hollow Prussian blue analogue (CoFe–PBA) nanocubes, using spherical silica particles as sacrificial templates. In the first step, silica cores are coated by a CoFe–PBA shell and then removed by etching with hydrofluoric acid (HF). The cubic shape of CoFe–PBA is well-retained even after the removal of the silica cores, resulting in the formation of hollow CoFe–PBA cubes. The specific capacity of the hollow CoFe–PBA nanocubes electrodes is about two times higher than that of solid CoFe–PBA nanocubes as storage materials for sodium ions. Such an improvement in the electrochemical properties can be attributed to their hollow internal nanostructure. The hollow architecture can offer a larger interfacial area between the electrolyte and the electrode, leading to an improvement in the electrochemical activity. This strategy can be applied to develop PBAs with hollow interiors for a wide range of applications.

1. Introduction

Coordination polymers, including porous coordination polymers (PCPs) and metal-organic frameworks (MOFs), have undergone extensive research in recent times. Such studies attract interest in industrial chemistry, materials science, and engineering. The functionality and the regularity of the shapes and sizes of PCPs and MOFs make them useful in separation, storage, catalysis, and so forth.[1–4] Their compositions can be generalized as $A_xM'_y[M''_z(CN)_6]$, where A is an alkali metal cation, M′ and M″ are transition metal cations, and the subscripts (*x*, *y* and *z*) express non-stoichiometry (or lattice defects), depending also on the valence of the transition metal(s). Their properties can be tuned by selecting the transition-metal cations. When M′ = M″ = Fe, the final composition will be $Fe_4[Fe(CN)_6]_3{\cdot}xH_2O$, which is generally known as Prussian Blue (PB). PB and PB analogues (PBAs) represent a well-known group of coordination polymers (CPs), where cyanide groups act as bridges between the transition metal ions (M^{2+}–CN–M^{3+}).[5,6] Moreover, various PBA nanocubes were synthesized recently in solutions through a controlled crystal growth process.[7] Roy et al. demonstrated the formation of a mesostruc-

[a] A. Azhar,[+] Dr. M. B. Zakaria,[+] Prof. J. Lin
College of Chemistry and Molecular Engineering
Qingdao University of Science and Technology
Qingdao 266042 (P. R. China)
E-mail: mohamed.hegazy3@science.tanta.edu.eg
iamjjlin@njtech.edu.cn

[b] A. Azhar,[+] Dr. M. B. Zakaria,[+] Prof. T. Chikyow, Prof. Y. Bando, Dr. Z.-X. Cai
International Research Center for Materials Nanoarchitechtonics
(WPI-MANA), National Institute for Materials Science (NIMS)
1-1 Namiki, Tsukuba, Ibaraki 305-0044 (Japan)

[c] A. Azhar[+]
Faculty of Science and Engineering, Waseda University
3–4-1 OkuboShinjuku, Tokyo, 169–8555 (Japan)

[d] Dr. M. B. Zakaria,[+] Prof. E. M. Ebeid
Department of Chemistry, Faculty of Science
Tanta University, Tanta, Gharbeya 31527 (Egypt)

[e] Prof. A. A. Alshehri, Prof. Y. G. Alghamdi
Department of Chemistry, King Abdulaziz University
P.O. Box. 80203, Jeddah 21589 (Saudi Arabia)

[f] Dr. N. A. Kumar, Prof. Y. Yamauchi
School of Chemical Engineering and Australian Institute for
Bioengineering and Nanotechnology (AIBN)
The University of Queensland, Brisbane, QLD 4072 (Australia)
E-mail: y.yamauchi@uq.edu.au

[g] Prof. H. Kim
Department of Energy Engineering, Hanyang University
Seongdong-gu, Seoul 133–791 (Republic of Korea)
E-mail: khansu@hanyang.ac.kr

[h] Prof. Y. Yamauchi
Department of Plant & Environmental New Resources
Kyung Hee University, 1732 Deogyeong-daero, Giheung-gu
Yongin-si, Gyeonggi-do 446–701 (Republic of Korea)

[+] These authors contributed equally to this work

Supporting Information and the ORCID identification number(s) for the author(s) of this article can be found under: https://doi.org/10.1002/open.201800120.

tured PB framework using a ligand-assisted templating approach in formamide.[8] Other PBAs with various morphologies (e.g. nanowires, nanocubes, nanospheres, and nanotubes) have been reported through different methods such as sonochemical, hydrothermal, electrodeposition, and microwave-assisted methods.[9] Dual-textured PB cubes with nanoporous shells are also reliable electrode materials for sodium-ion storage.[10] Taking advantage of their hybrid nanostructures composed of porous and non-porous domains, dual-textured PB cubes exhibit high reversible capacities, good rate capabilities, stable cyclic performances, and excellent dimensional stabilities even after several charge–discharge cycles, offering new opportunities for the development of robust and high-performance rechargeable sodium-ion batteries.

Although several PB and PBA nanostructures have been reported, hollow PBAs have attracted great interests because of their enhanced physical and chemical properties. For example, Maurin-Pasturel et al. reported the synthesis of hollow NiFe–PBA nanoparticles using gold nanoparticles as a sacrificial template.[11] By simply dispersing the core–shell Au@NiFe–PBA in KCN solution, hollow NiFe–PBA could be obtained, because of the intrinsic porosity of the PBA network. In addition, Risset et al. demonstrated a facile surfactant-free route to synthesize uniform $Rb_{0.4}M_4[Fe(CN)_6]_{2.8}\cdot 7.2H_2O$ (M = Co, Ni) hollow nanoparticles.[12] To the best of our knowledge, to date, only one effective method for the preparation of crystalline hollow PBA nanoparticles by etching with HCl under hydrothermal conditions has been demonstrated.[13] Our previous study reported the preparation of hollow PBA cubes by using another PBA sacrificial core followed by removal through a chemical treatment.[14] By investigating the electrochemical performance of solid and hollow CoCo–PBA cubes, it was demonstrated that hollow CoCo–PBA cubes exhibited a higher surface area, which is the significant advantage of a hollow structure for providing more oxidation and reduction reaction sites for a better performance in energy storage applications.

For the above nanostructures, a hollow structure is ideal for electrode materials in lithium- and sodium-ion batteries, because the unique nature of a hollow nanostructure can offer a more favorable path for the electrolyte and enlarge the electrochemically active surface area of the electrode materials, thereby improving the electrochemical kinetics. In this paper, we demonstrate the facile synthesis of hollow CoFe–PBA cubes, using spherical silica cores as sacrificial templates. Recently, silica nanoparticles were used as hard templates, because they possess silanol groups on their surface, which induce the formation reaction of many shells on the surface of silica.[15] Also, it is possible to control the size and the shape of the hollow interiors without consideration of complicated reactions. This method can be applicable to PB and PBA systems for hollow inorganic nanostructures, as shown in this work.

2. Results and Discussion

The synthetic scheme for the hollow CoFe–PBA nanocubes is shown in Figure 1. First, the CoFe–PBA grew on the spherical silica particle. After the reaction was complete, the SiO_2@CoFe

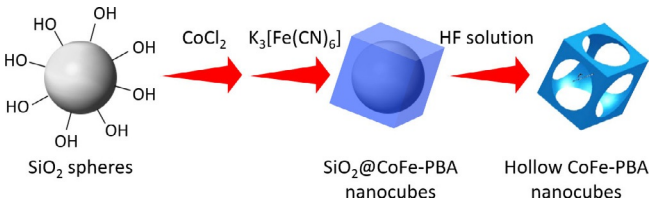

Figure 1. Schematic illustration of the formation of hollow CoFe–PBA using silica spheres as sacrificial templates.

precipitate was collected by centrifugation and washing with water and ethanol. Finally, the SiO_2 cores were removed by etching, using HF solution to prepare the hollow CoFe–PBA cubes. The morphology and size of the silica spheres, core–shell SiO_2@CoFe–PBA cubes, and hollow CoFe–PBA cubes were investigated by using scanning electron microscopy (SEM) and transmission electron microscopy (TEM) (Figure 2). Spherical

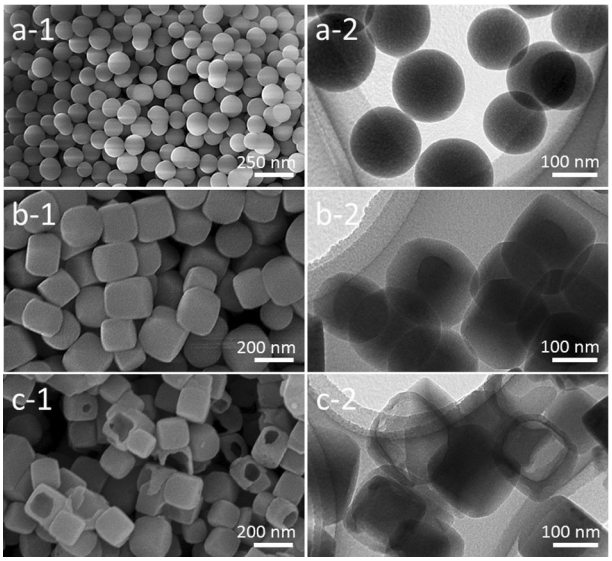

Figure 2. SEM (1) and TEM (2) images of a) silica spheres, b) SiO_2@CoFe–PBA, and c) hollow CoFe–PBA cubes.

silica particles of around 150 nm in diameter were used as the template (Figure 2a). After coating with the CoFe–PBA shell, the average particle size became around 200 nm (Figure 2b), indicating that the shell thickness is around 50 nm. After removal of the silica template, hollow CoFe–PBA cubes were obtained (Figure 2c). The hollow interior was more than 150 nm in diameter, which was larger than the size of the starting silica particles. This is because the etching agent still works even after the removal of silica particles, resulting in the formation of a larger cavity than expected.

Figure 3 shows wide-angle XRD patterns for silica spheres, solid CoFe PBA, core–shell SiO_2@CoFe–PBA cubes, and hollow CoFe–PBA cubes. A broad diffraction peak was noticed from 15 to 30°, which was assigned to silica. The XRD patterns of the core–shell SiO_2@CoFe–PBA cubes and the hollow CoFe–PBA cubes showed the same diffraction patterns of the solid CoFe–PBA, which could be attributed to the face-centered-

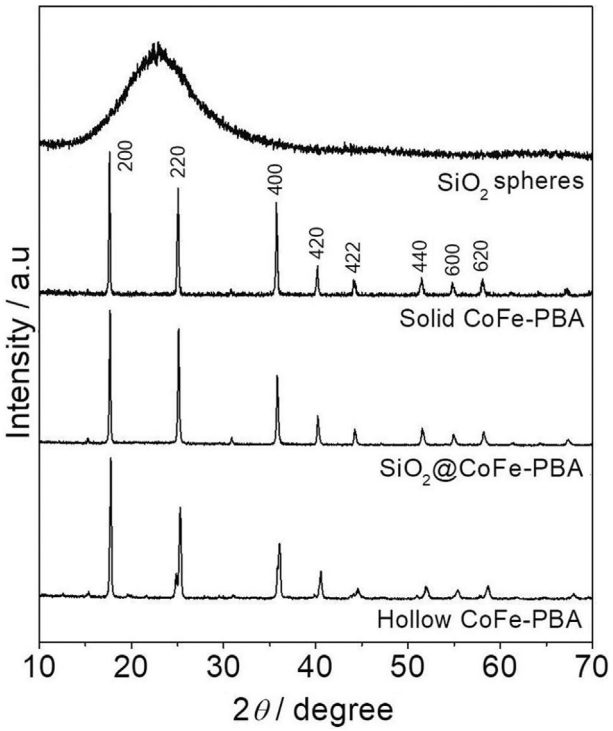

Figure 3. Wide-angle XRD diffraction patterns for silica spheres, solid CoFe–PBA, SiO_2@CoFe–PBA, and hollow CoFe–PBA cubes.

cubic crystal structure with the *Fm*3*m* unit cell. The XRD diffraction peaks of the hollow CoFe–PBA become a little broad, owing to a decrease in the original crystallinity of CoFe–PBAs. However, the crystal structure is preserved even after the removal of the silica cores.

The FTIR spectrum of as-prepared core–shell SiO_2@CoFe–PBA is shown in Figure S1. The band at 2114 cm^{-1} could be indexed to the CN stretching (Co^{III}–NC–Fe^{II}),[16] whereas the band at 1110 cm^{-1} could be assigned to the Si–*O*–Si vibration.[17] Figures S2 and S3 show the XRD patterns of as-prepared CoFe–PBA and core–shell SiO_2@CoFe–PBA. The Pawley fitting of these XRD patterns shows that the structure of each sample is in the same space group. The structural and crystallographic details are provided in Table S1. These data indicate the successful coating of CoFe–PBA on the silica spheres.

Recently, lithium-ion batteries (LIBs) and sodium-ion batteries (SIBs) with PB and PBAs as electrode materials have been widely explored.[18,19] Owing to the high abundance and suitable redox potential, SIBs are considered possible replacements for LIBs, especially for applications in large energy storage devices.[20] It is widely accepted that the nanostructure of materials holds the key to their electrochemical reactivity.[21,22] In this context, PB and PBAs offer a solution, because they possess a three-dimensional open framework with large interstitial sites for a high rate of mass transfer toward alkali cations that can improve their cycle performance at high currents.[18,19] In particular, the hollow structure is known to improve the electrochemical properties of electrode materials in LIBs and SIBs, as the unique nature of hollow microstructures can offer a more favorable pathway for the electrolyte and enlarge the electrochemically active surface area of electrode materials. Thus, to understand the effect of the nanostructure modification of CoFe–PBA on the electrochemical sodium-ion storage characteristics, solid and hollow CoFe–PBA materials were investigated as cathode materials for SIBs.

Figure 4a shows the voltage profiles of solid and hollow CoFe–PBA cathodes for SIBs. Even though their capacities were relatively low compared to that of other PBA cathodes in previous reports,[23,24] we clearly found that the hollow nanostructure could significantly improve the sodium-ion storage characteristics of CoFe–PBA cathode materials. Although the solid CoFe–PBA electrode showed just 12.5 mAh g^{-1} in the first cycle, the hollow structured CoFe–PBA electrode showed reversible capacities that were approximately two times higher than the non-treated solid homologue in the same cycle. The inset of Figure 4a shows the differential capacity plots (DCPs) of solid and hollow CoFe–PBA electrodes for the first cycle. Upon the charging process, the DCP peak of the hollow CoFe–PBA electrode was observed at a lower potential (3.30 V vs. Na/Na^+) than that of solid CoFe–PBA (3.38 V vs. Na/Na^+). This result combined with the much-improved capacity of hollow CoFe–PBA clearly reveals that nanostructure modification can

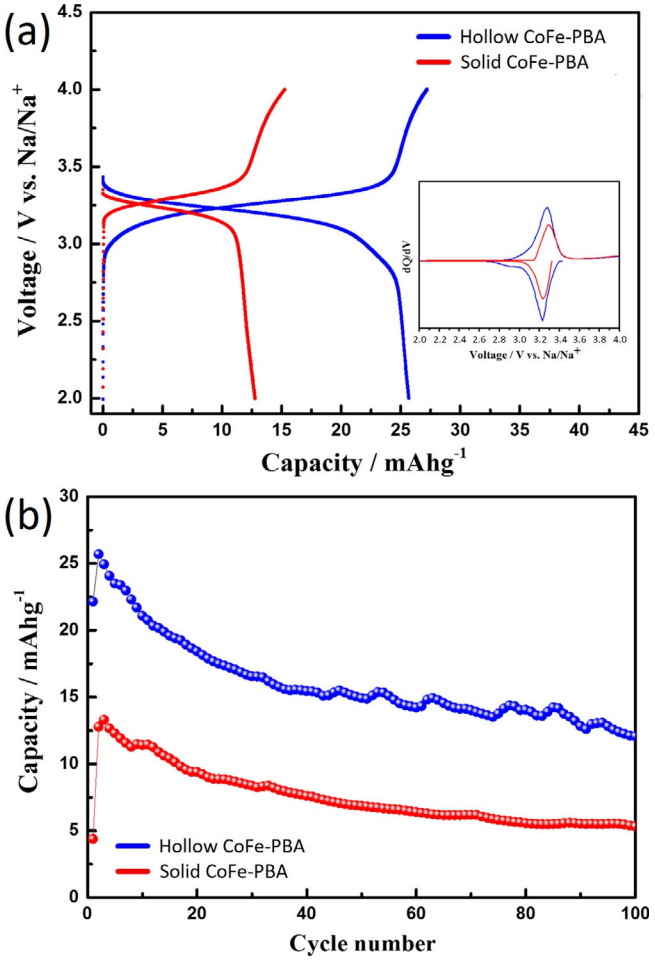

Figure 4. a) Voltage profiles obtained during the initial two cycles (inset: differential capacity plots) and b) cycle performance of solid and hollow CoFe cubes.

reduce the overpotential of the CoFe–PBA electrode during cycling. Such an improvement in the hollow CoFe–PBA cathode can be explained by the aforementioned nanostructure, which is highly favorable for electrochemical sodium-ion insertion and removal in CoFe–PBA. As shown in Figure 4b, hollow CoFe–PBA electrode shows fairly stable cycle performance during cycling without significant decrease in the capacity, which is almost double that of the untreated solid CoFe–PBA electrode. This result suggests that the hollow structuring of CoFe–PBA does not have a negative influence on the reliability of repeated sodium-ion insertion and removal process over 100 cycles.

3. Conclusions

We demonstrated the formation of hollow CoFe–PBA nanocubes by using silica spheres as hard templates and examined their feasibility as cathode materials for SIBs. The silanol groups on the surface of the silica spheres reacted with cobalt cations in the first step. Nucleation of CoFe–PBA started simultaneously upon addition of iron cyanide ligands in the second step. After aging overnight, a thin shell of CoFe–PBA was successfully formed on the surface of the silica spheres. Silica cores were then removed by chemical etching, yielding hollow CoFe–PBA nanocubes. The hollow nanostructure of CoFe–PBA nanocubes helps to improve the storage capacity of sodium ions with stable cycle performance compared to the solid CoFe–PBA nanocubes. We strongly believe that our synthetic approach will be useful in the future for the formation of various PB and PBAs with open frameworks, high specific surface area, improved storage capacity, and stable cycle performance at high currents for SIBs.

Experimental Section

Chemicals

Tetraethyl orthosilicate (TEOS, 99 wt%) and potassium hexacyanoferrate (III) hydrate were purchased from Sigma–Aldrich, USA. Ammonium hydroxide solution (NH_4OH, 25 wt%), hydrofluoric acid (HF, 10 wt%), trisodium citrate dihydrate (TSCD), and cobalt (II) chloride anhydrous ($CoCl_2$) were purchased from Nacalai Tesque, Inc., Japan. All reagents were used without further purification.

The spherical silica particles were prepared according to Stöber's method. In these procedures, 21 mL of tetraethyl orthosilicate (TEOS, 99 wt%), 9 mL of deionized water, and 245 mL of NH_4OH solution (25 wt%) were added to 225 mL of ethanol and stirred at room temperature for 4 h. A white colloidal solution of silica particles was obtained. The silica particles were separated by centrifugation, washed by ethanol for four times, and dried under ambient conditions at room temperature.

Synthesis of Hollow CoFe–PBA

The previously prepared spherical silica particles (20 mg) were dispersed in a mixture consisting of cobalt chloride anhydrous (77.9 mg) and TSCD (397.1 mg) dissolved in distilled water (20 mL) to form solution A. At this stage, the surface of the silica particles was decorated with Co ions after interaction with the silanol groups. Meanwhile, potassium hexacyanoferrate (III) hydrate (133 mg) was dissolved in pure water (20 mL) to form clear solution B. Then, solutions A and B were mixed together whilst stirring followed by aging for 4 days. The SiO_2@CoFe–PBA precipitate was collected by centrifugation and washing with water and ethanol several times. After drying at room temperature overnight, the SiO_2 cores were removed by etching with HF. SiO_2@CoFe–PBA (40 mg) was suspended in 10% HF solution (25 mL) by stirring for 12 h to complete the silica removal. The hollow CoFe–PBA precipitate was collected by centrifugation and washing with water and ethanol several times, which was dried at room temperature for 24 h.

Structural Characterization

A field-emission scanning electron microscope (FESEM; JEOL JSM-7000F) and high-resolution transmission electron microscope (HRTEM; JEOL ARM-200F) were employed to characterize the morphology and the nanostructure. X-ray diffraction (XRD; Rigaku RINT 2500X diffractometer) patterns were obtained by using monochromated Cu Kα radiation (40 kV, 40 mA) at a scanning rate of 1° min^{-1}. The XRD data were collected in the 2θ range of 10–70° under ambient conditions. The lattice parameters were refined by the Pawley method, using the GSAS-II software,[25] and the zero shifts of the patterns were corrected with background subtraction. The result of the fitting method was identical to the crystal structure of $K_2Co[Fe(CN)_6]$ (CCDC 28669). Fourier transform infrared spectroscopy (FTIR) of a KBr pressed pellet sample was carried out by using a Thermoscientific Nicolet 4700 instrument, and the data were collected in the range of 500 to 4000 cm^{-1} at room temperature.

Electrochemical Measurements

The slurries were manufactured by mixing the active materials (80 wt%), Super-P as a conducting agent (10 wt%), and poly(acrylic acid) dissolved in deionized water as a binder (10 wt%) with deionized water. To prepare the working electrodes, the obtained slurries were coated onto Al foil as a current collector. The electrodes were dried at 80 °C for 30 min in a convection oven to evaporate the water, and were then heat-treated at 120 °C overnight under vacuum. The cells were assembled by using CR2032 coin-type half cells with sodium metal as a counter electrode, glass fiber (GF/F; Whatman) as a separator, and 0.7 M $NaClO_4$ dissolved in a mixed solvent of ethylene carbonate (EC) and diethyl carbonate (DEC) (1:1, v/v; Panax Etec Co. Ltd.) as the electrolyte in an Ar-filled glove box. The cells were galvanostatically charged and discharged at a constant current (CC) within the voltage window of 2.0–4.0 V versus Na/Na^+ at 10 mA g^{-1} at room temperature.

Acknowledgements

M.B.Z. acknowledges financial support from Japan Society for the Promotion of Science (JSPS). This work was supported by the Deanship of Scientific Research (DSR), King Abdulaziz University (Grant number KEP-7–130-39), an Australian Research Council (ARC) Future Fellow (Grant number FT150100479), JSPS KAKENHI (Grant numbers 17H05393 and 17K19044), and the research fund by the Suzuken Memorial Foundation. This work was also supported by the National Natural Science Foundation of China (NSFC) (61604070), the Natural Science Foundation of the Higher Education Institutions of Jiangsu Province (16KJB430015), the Na-

tional Natural Science Foundation of Jiangsu Province (BK20161000), and the Jiangsu Six Talent Plan.

Conflict of Interest

The authors declare no conflict of interest.

Keywords: batteries · coordination polymers · crystal growth · hollow structures · Prussian blue analogues

[1] F. Debatin, A. Thomas, A. Kelling, N. Hedin, Z. Bacsik, I. Senkovska, S. Kaskel, M. Junginger, H. Müller, U. Schilde, *Angew. Chem. Int. Ed.* **2010**, *49*, 1258 – 1262; *Angew. Chem.* **2010**, *122*, 1280 – 1284.
[2] J. Heine, K. Müller-Buschbaum, *Chem. Soc. Rev.* **2013**, *42*, 9232 – 9242.
[3] Y. B. Huang, J. Liang, X. S. Wang, R. Cao, *Chem. Soc. Rev.* **2017**, *46*, 126 – 157.
[4] D. Tanaka, A. Henke, K. Albrecht, M. Moeller, K. Nakagawa, S. Kitagawa, J. Groll, *Nat. Chem.* **2010**, *2*, 410 – 416.
[5] M. B. Zakaria, A. A. Belik, C. H. Liu, H. Y. Hsieh, Y. T. Liao, V. Malgras, Y. Yamauchi, K. C. W. Wu, *Chem. Asian J.* **2015**, *10*, 1457 – 1462.
[6] S. Adak, L. L. Daemen, M. Hartl, D. Williams, J. Summerhill, H. Nakotte, *J. Solid State Chem.* **2011**, *184*, 2854 – 2861.
[7] M. Hu, S. Ishihara, K. Ariga, M. Imura, Y. Yamauchi, *Chem. Eur. J.* **2013**, *19*, 1882 – 1885.
[8] X. Roy, L. K. Thompson, N. Coombs, M. J. MacLachlan, *Angew. Chem. Int. Ed.* **2008**, *47*, 511 – 514; *Angew. Chem.* **2008**, *120*, 521 – 524.
[9] M. B. Zakaria, T. Chikyow, *Coord. Chem. Rev.* **2017**, *352*, 328 – 345.
[10] D. S. Kim, M. B. Zakaria, M.-S. Park, A. Alowasheeir, S. M. Alshehri, Y. Yamauchi, H. Kim, *Electrochim. Acta* **2017**, *240*, 300 – 306.
[11] G. Maurin-Pasturel, J. Long, Y. Guari, F. Godiard, M. G. Willinger, C. Guerin, J. Larionova, *Angew. Chem. Int. Ed.* **2014**, *53*, 3872 – 3876; *Angew. Chem.* **2014**, *126*, 3953 – 3957.
[12] O. N. Risset, E. S. Knowles, S. Ma, M. W. Meisel, D. R. Talham, *Chem. Mater.* **2013**, *25*, 42 – 47.
[13] M. Hu, S. Furukawa, R. Ohtani, H. Sukegawa, Y. Nemoto, J. Reboul, S. Kitagawa, Y. Yamauchi, *Angew. Chem. Int. Ed.* **2012**, *51*, 984 – 988; *Angew. Chem.* **2012**, *124*, 1008 – 1012.
[14] M. B. Zakaria, M. Hu, M. Imura, R. R. Salunkhe, N. Umezawa, H. Hamoudi, A. A. Belik, Y. Yamauchi, *Chem. Eur. J.* **2014**, *20*, 17375 – 17384.
[15] A. Thomas, F. Goettmann, M. Antonietti, *Chem. Mater.* **2008**, *20*, 738 – 755.
[16] G. Fornasieri, M. Aouadi, P. Durand, P. Beaunier, E. Rivière, A. Bleuzen, *Chem. Commun.* **2010**, *46*, 8061 – 8063.
[17] J. Manokaran, R. Muruganantham, A. Muthukrishnaraj, N. Balasubramanian, *Electrochim. Acta* **2015**, *168*, 16 – 24.
[18] J. Peng, J. Wang, H. Yi, W. J. Hu, Y. Yu, J. Yin, Y. Shen, Y. Liu, J. Luo, Y. Xu, P. Wei, Y. Li, Y. Jin, Y. Ding, L. Miao, J. Jiang, J. Han, Y. Huang, *Adv. Energy Mater.* **2018**, *8*, 1870048.
[19] Y. Lu, L. Wang, J. Cheng, J. B. Goodenough, *Chem. Commun.* **2012**, *48*, 6544 – 6546.
[20] C. Vaalma, D. Buchholz, M. Weil, S. Passerini, *Nat. Rev. Mater.* **2018**, *3*, 18013.
[21] J. Ye, W. Liu, J. Cai, S. Chen, X. Zhao, H. Zhou, L. Qi, *J. Am. Chem. Soc.* **2011**, *133*, 933 – 940.
[22] M. Okubo, E. Hosono, J. Kim, M. Enomoto, N. Kojima, T. Kudo, H. Zhou, I. Honma, *J. Am. Chem. Soc.* **2007**, *129*, 7444 – 7452.
[23] J. Qian, C. Wu, Y. Cao, Z. Ma, Y. Huang, X. Ai, H. Yang, *Adv. Energy Mater.* **2018**, *8*, 1702619.
[24] X. Bie, K. Kubota, T. Hosaka, K. Chihara, S. Komaba, *J. Power Sources* **2018**, *378*, 322 – 330.
[25] B. H. Toby, R. B. Von Dreele, *J. Appl. Crystallogr.* **2013**, *46*, 544 – 549.

Received: June 25, 2018

